Received: 22 December 2021 | Revised: 13 May 2022 | Accepted: 12 June 2022

DOI: 10.1002/ep.13936

ENVIRONMENTAL PROGRESS & SUSTAINABLE ENERGY

ORIGINAL RESEARCH

Sustainable Energy

Experimental and numerical engine cycle setup for a dual fuel hydrogen, methane, and hythane with diesel to assess the effect of water injection and nozzle geometry

Hadi Taghavifar

Department of Technology and Safety, UiT the Arctic University of Norway, Tromsø, Norway

Correspondence
Hadi Taghavifar, Department of Technology and Safety, UiT the Arctic University of Norway, Tromsø, Norway.
Email: haditaghavifar@yahoo.com

Abstract

In this study, the potential of gaseous fuels such as hydrogen, methane, and hythane in combination with diesel fuel is assessed in a closed loop thermodynamic framework. An experimental test is conducted with basic diesel fuel and then the model is configured based on the realistic one-cylinder diesel engine to evaluate the robustness and reliability of the simulation. The model is accurate in terms of in-cylinder pressure, temperature, and heat release rate within the 3% error band. In principle, three blend cases of diesel50%—methane50%, diesel50%—hydrogen50%, and diesel50%—hythane50% are compared with baseline neat diesel from engine performance to emissions characteristics. For hythane and hydrogen-involved fuels, the 10% water injection effect is analyzed as well to damp the high flammability and ignition intensity of hydrogen. The findings indicate that the entropy generation in hythane and hydrogen is markedly higher than in diesel case, while water injection can slightly decrease the entropy amount. It is shown that D50H50 has more fuel consumption in higher nozzle diameter (28% at 1 mm hole diameter), while in lower nozzle size range pure diesel fuel consumption dominates. The results revealed that D50Hy40W10 is particularly effective for elevated torque at lower nozzle hole values since the steam contributes toward maximized pressure and the exerted force. The increase of the nozzle number resulted in the CO content increase in the exhaust with the burning temperature reduction.

KEYWORDS
1D thermodynamic modeling, hydrogen enrichment, hythane fuel, nozzle hole, water injection

1 | INTRODUCTION

Hydrogen-based engines are in the spotlight with much attention given to developing the feasibility and operability of such schemes. Methane or natural gas is an alternate fuel that provides a robust framework for green energy and clean combustion concept in internal combustion engines. The environmental challenges worldwide enforce the research and development of automobile industries to comply with progressively more stringent policies on pollutant emissions regulations by keeping the smoke, NO_x, and CO_2 within the permissible threshold of Euro 5 standards in the majority of developed countries.[1–3]

Hydrogen as a promising energy vector is envisaged to be utilized in the fuel cell segment of hybrid electric vehicles as well as in internal combustion engines either as a premixed mode or direct injection approach.[4,5] Alternatively, methane and hydrogen–methane (hythane) are gaseous fuels with both high energy density and clean/green energy sources that can mitigate global warming and the greenhouse effect.[6] The outlook of the automotive industry navigates through a promising future where hydrogen can be more affordable, cost-effective, economic, and sustainable although there are serious concerns over infrastructure and storage concerns to various reports from EEA to EPA and EU.[7,8]

In the recent years, there are research projects that investigated the use of hydrogen in proportion blended with other fuels in both SI and CI engines, where the target is set to reduce the emissions below the limit while simultaneously producing high power output. It is approved that hydrogen addition can extend the flammability limit, and contribute to faster flame propagation, and lean-burn capacity in the cylinder,[9] while boosting the thermal efficiency with NO_x decline.[10] In this context, Gong et al.[11] explored the effect of hydrogen addition to methanol-fueled SI engines to observe the trend in ignition timing, combustion quantities, and emissions variation. The outcome of the tests indicated increased indicated mean effective pressure (IMEP), maximum cylinder pressure, and heat release rate (HRR) with hydrogen addition at both low and high engine speeds. The levels of NO_x and soot, however, increased with hydrogen addition at high engine speeds. Yip et al.[12] reviewed comprehensively the direct injection of hydrogen in an attempt to picture a carbon-free prospective for ICEs. According to this study, hydrogen is beneficial for the design of effective engines since the diffusion of hydrogen is four times that of CNG, which is highly desirable for achieving a uniform mixture or charge. The optimization technique can be applied for the engine cycle and gas exchange modeling to find the best operational condition of the diesel engine to manage the emission and increase the energy efficiency.[13] The regulation of air/fuel mixing, swirl motion, compression ratio, and coolant temperature are taken as design variables to reach the best solution meeting the objective function desirable amount. The powertrain simulation aids toward fuel flow and injection or air mixing mechanism understanding especially when it comes to the reactivity controlled compression ignition (RCCI) concept. This has been practiced in Reference 14, where the hydrogen and diesel fuels are introduced to the chamber as port induction and direct injection. This allows for in-depth energy, exergy, and performance analysis of the power drive unit. Recently, Subramanian et al.[15] have gone through a comprehensive study on different energy fractions of hydrogen and oxygen gas (HHO) in a dual-fuel engine. By using this gas, the thermal brake efficiency has increased significantly, while the specific fuel consumption as well as CO_2, HC, and NO_x emissions reduced.

The 1D calculation software of AVL boost furnishes a proper platform for simulation of engine component connection and thermodynamic modeling of conservation equations and combustion kinetics of in-cylinder processes. This potent code is employed by Karagoz et al.[16] for studying the effect of hydrogen addition on combustion and emission features of spark-ignited engines. Both the Woschni heat transfer and Vibe 2-zone combustion models are considered to account for detailed engine results under different engine speeds and lambda values. The obtained results explain why CO and total hydrocarbons (THC) decrease while NO_x increases with the use of hydrogen as a fuel in the SI engine. Similarly, Ayad et al.[17] performed a hydrogen-enriched ethanol-fueled SI engine simulation on the same platform. The findings are highlighted with better thermal efficiency at low boost for pure ethanol, whereas at high boost situation, hydrogen-enriched cases lead to better thermal efficiency. In an experimental study conducted by Sandalci et al.,[6] the impact of hythane enrichment is explored for its viability in a CI engine in terms of performance and emission. They proposed a solution to obviate the dieselization issue when hythane is applied in a diesel engine in dual-fuel operation. However, hythane addition leads to increased CO, NO_x, and THC, though it also results in the rise of maximum cylinder pressure and HRR. Niculae et al.[18] conducted a simulation study of SI operated engine with alternative fuels in the gaseous form of CNG (100% methane), different hythane blends, and hydrogen. Their results indicate higher engine efficiency, and reduced THC, CO, and NO_x when replacing gasoline with hythane.

TABLE 1 Engine specifications

Engine specs	Value/comment
Manufactured	Opex company
Rated brake power	8/5.9 (bhp/kW)
Rated speed	1500 (rpm)
Number of cylinders	1
Bore × Stroke	87.5 × 110 (mm)
Compression ratio	17.5:1
Cooling sys	Water cooled
Lubrication sys oil	SAE 30/SAE 40
Injection opening pressure	220 (bar)

One of the methods to control detonation and/or knocking in the engines with hydrogen injection is to apply water injection, which is also employed in our study. Xu et al.[19] analyzed the effect of water injection in the hydrogen-fueled spark-ignited engine while the excess air ratio and spark timing were varied. They found a considerable NO_x drop and a slight increase of indicated mean effective pressure (IMEP) with water-to-air ratio increment.

This study complements experimental and numerical approaches to study the effect of different diesel-based fuels blended with methane, hydrogen, and hythane with/without water involvement under the influence of operational factors of nozzle-hole, number of nozzles, compression ratio, and engine speed. The experimental test is designed with a single-cylinder diesel engine with diesel fuel at full load and 1500 rpm speed. After calibration of the test rig, the corresponding data are used in AVL Boost; while appropriate combustion, emission, water cooling, and heat transfer models are adopted and a successful validation is achieved.

Based on the reviewed literature, there has been a gap in diesel engine analysis with hydrogen, methane, and hythane with water addition, when the injection parameters are included. The present investigation attempts to introduce the best composition of fuel for each of the engine performance and emission reduction strategies.

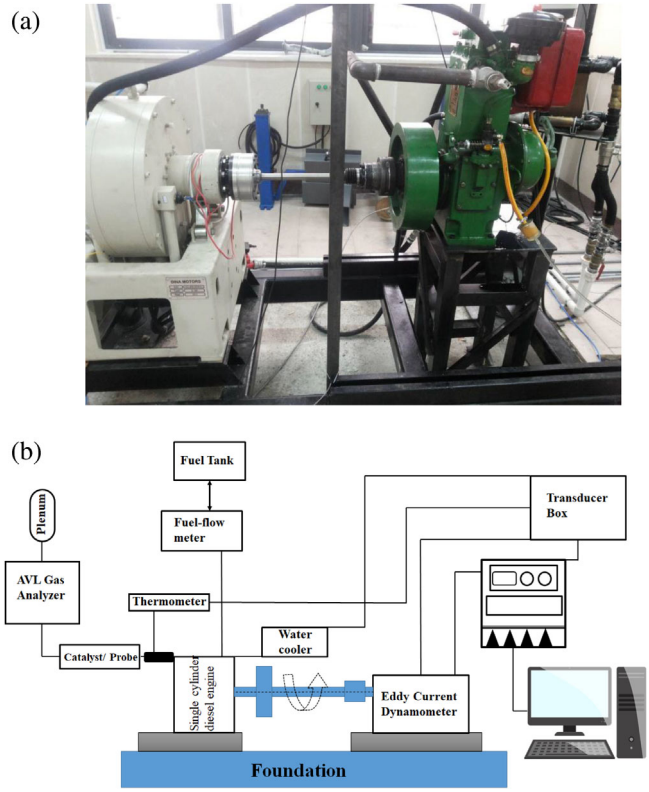

FIGURE 1 (a) Experimental test rig, (b) a schematic view of the setup

2 | EXPERIMENTAL DETAILS

A direct injection compression ignition engine, whose characteristics are given in Table 1, was utilized in the experiment. It is a single-cylinder, water-cooled engine as shown in Figure 1. An eddy current dynamometer coupled through a shaft was used to deduce the brake power of the engine during operation. The engine-out emission species were quantified using an AVL Di Gas analyzer unit, which was connected to the tailpipe after the catalyst but before the plenum. Short running intervals were implemented to reduce transient emission fluctuations. The FTO flow meter manufactured by Flowtech Company was employed to monitor the flow rate of the fuel. The measurement uncertainty and reliability index for the experimental rig components were estimated following Reference 20:

Engine speed ±1 rpm, engine torque ±1 Nm, NO_x emissions ±5%, CO emissions ±1%, CO_2 emissions ±2%, HC emissions ±2%, smoke ±5%, fuel flow rate measurement ±1%, and lower heating value of the fuel ±4%.

In order to assure the reliability of the tests with the reference diesel fuel and to have confidence in the repeatability of the experiment, the engine runs on diesel fuel under full load and at 1500 rpm for 15 min for the engine warm-up and to reach the stabilized situation. The tests are repeated and the obtained data having lesser than ±0.02 error is taken for reporting, after finishing the procedure, the tank and fuel line is cleansed.

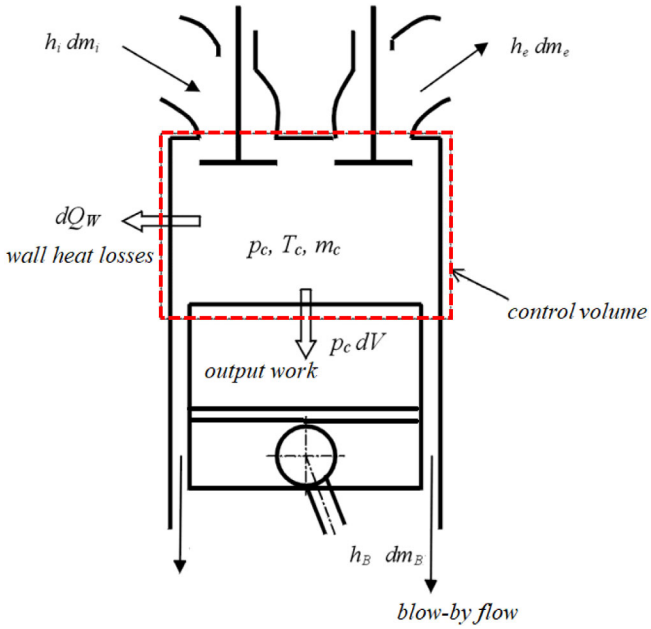

FIGURE 2 A schematic sketch of cylinder.

3 | NUMERICAL FORMULATION OF 1D ENGINE SIMULATION

The AVL Boost interface is employed for modeling the different components and the fundamental process of combustion, mass/species transport, momentum, energy/heat transfer. The system configuration is an assembly of variety of components such as air-cleaner, cooling heat exchanger, cylinder, catalyst, and plenums.

3.1 | Governing equations

According to the first law of thermodynamics, and considering the moving control volume within the piston-cylinder arrangement, the state of the system based on crank-angle is estimated as[21]:

$$\frac{d(m_c.u)}{d\theta} = -p_c.\frac{dV}{d\theta} + \frac{dQ_F}{d\theta} - \sum\frac{dQ_w}{d\theta} - h_B.\frac{dm_B}{d\theta} + \sum\frac{dm_i}{d\theta}.h_i - \sum\frac{dm_e}{d\theta}.h - q_{evp}.y.\frac{dm_{evp}}{dt} \quad (1)$$

The mass flow change with crank-angle is given as follows:

$$\frac{dm_c}{d\theta} = \sum\frac{dm_i}{d\theta} - \sum\frac{dm_e}{d\theta} - \frac{dm_B}{d\theta} + \frac{dm_{evp}}{dt} \quad (2)$$

where θ is crank-angle, p_c, m_c, V, u, y, and q_{evp} are, respectively, cylinder pressure, cylinder mass, volume, specific internal energy, fuel evaporation fraction, and evaporation heat. Referring to Equation (1), the variation in internal energy is the sum of piston work, fuel heat, wall heat losses, and outflow of enthalpy, respectively. The in-cylinder gas composition is determined from the immediate combustion of the

added fuel perfectly homogenized with the residual cylinder charge. Therefore, the air/fuel ratio decreases consistently from start of combustion onward until the end of combustion. The following equation, together with Equation (1), are employed to update pressure, temperature, and density using a Runge–Kutta method.

$$p_c = \frac{1}{V}.m_c.R_o.T_c \tag{3}$$

where R_o is the universal gas constant. Upon finding the cylinder temperature, the above equation can be solved for obtaining the cylinder pressure. Figure 2 presents a schematic of the cylinder for basic calculations of in-cylinder energy balance.

3.2 | Heat transfer and combustion modeling and computation

The in-cylinder heat transfers across the walls of the combustion chamber, including the cylinder head, the piston, and the cylinder liner, is calculated using

$$Q_{wi} = A_i.\alpha_w.(T_c - T_{wi}) \tag{4}$$

The heat transfer rate from the wall is represented by Q_{wi}, where "i" in the subscript is one of the three walls of the chamber. Moreover, A_i is the surface area of the respective wall, α_w being the heat transfer coefficient, and T_c with T_{wi} are the cylinder gas temperature and wall temperature. For the heat transfer coefficient, there are different models developed for different applications. The modified Woschni heat transfer model[22] for α_w gives a more accurate account of the heat transfer especially at part load operation:

$$\alpha_w = 130.D^{-0.2}.p_c^{0.8}.T_c^{-0.53}.\left\{c_1.c_m.\left[1+2\left(\frac{V_{TDC}}{V}\right)^2.IMEP^{-0.2}\right]\right\}^{0.8} \tag{5}$$

Here, D signifies the cylinder bore, c_m is the mean piston speed, c_u is the circumferential velocity, $c_1 = 2.28 + 0.308\frac{c_u}{c_m}$, V_{TDC} the cylinder volume at TDC position, and V is the actual volume; while IMEP is the indicated mean effective pressure.

The mixing controlled combustion (MCC) model[23,24] is utilized to treat the combustion processes in the combustion chamber of CIDI (compression-ignition, direct-injection) engines. Specifically,

$$\frac{dQ_{MCC}}{d\theta} = C_{comb}.f_1(m_F, Q_{MCC}).f_2(k,V). \tag{6}$$

Considering,

$$f_1(m_F, Q_{MCC}) = \left(m_F - \frac{Q_{MCC}}{LHV}\right).(w_{O_2})^{C_{EGR}} \tag{7}$$

$$f_2(k,V) = C_{rate}.\frac{\sqrt{k}}{\sqrt[3]{V}} \tag{8}$$

where Q_{MCC} denotes cumulative heat release during diffusion stage (kJ), C_{comb}, C_{EGR}, and C_{rate} are combustion, EGR influence, and mixing rate constants. In addition, k is the local density of turbulent kinetic energy (m^2/s^2), m_F is the vaporized fuel mass (kg), V is the cylinder volume (m^3), LHV signifies the lower heating value (kJ/kg) and w_{O2} is the available oxygen mass fraction at SOI.

TABLE 2 The operating parameters of components in the software

parameters	Value / unit
Coolant temperature	58.2°C
Inlet air temperature	95°C
Total air cleaner volume	3.1 L
Number of injector holes	6
Hole diameter	0.5 mm
Rail pressure	1500 bar
Discharge coefficient	0.54
Premixed combustion parameter	0.7
In-cylinder swirl ratio	2

4 | THE INVESTIGATION PROCEDURE AND VALIDATION

In the first stage, the diesel fuel is tested on the experimental test bench at 1500 rpm and at full load condition, which is cooled by a

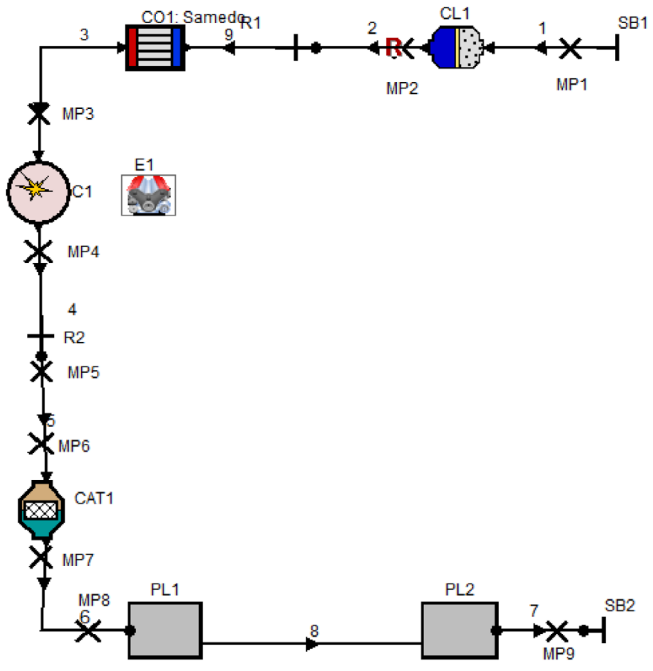

FIGURE 3 1D model of AVL Boost for engine line simulation

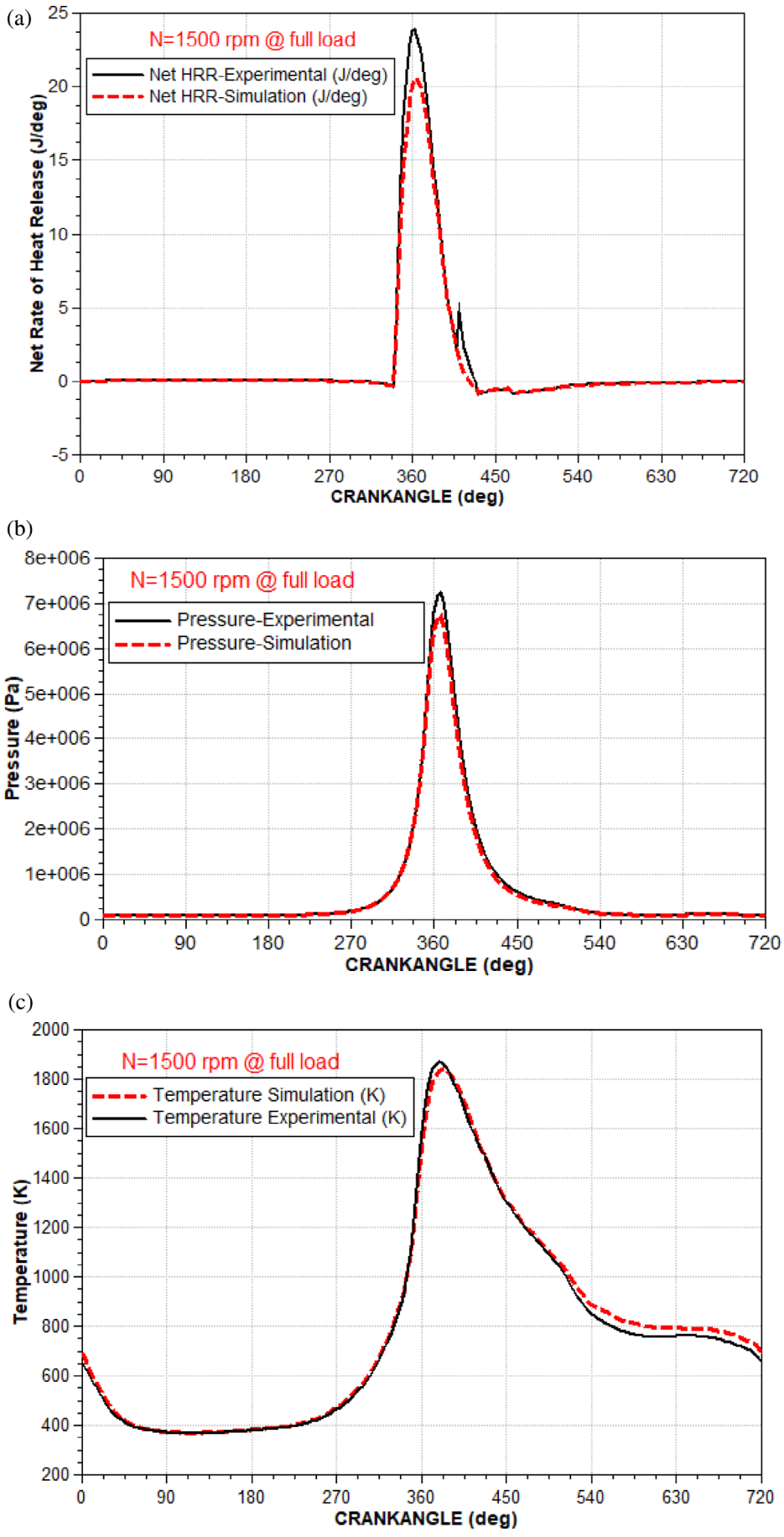

FIGURE 4 Comparison of experimental and numerical curves, (a) HRR, (b) pressure, and (c) temperature at 1500 rpm and full load for diesel engine

TABLE 3 Major fuel properties, fuel compositions, and related thermodynamic values

# Fuels	A/F ratio (–)	LHV (kJ/kg)	Molar mass (kg/kmol)	Heat of evaporation (J/kg)	Carbon/total mass ratio (–)
Diesel	15.1	42830.4	100.2	275,000	0.839
Methane	17.22	50044.7	16.04	513,000	0.748
Hydrogen	34.27	120043.1	2.01	456,000	0
Diesel50Methane 50	16.1	46437.5	58.1	394,000	0.793
Diesel50Hythane50 (50%Diesel-30% Methane-20%H_2)	21.3	67437.06	55.3	382,600	0.643
Diesel50Hydrogen50	24.7	81436.7	51.1	365,500	0.419

water cooler tool. Thereafter, the 1D simulation is performed by AVL Boost to model the engine line from the inlet air filter and water cooler to the cylinder and plenums. The modeling parameters such as cylinder bore, stroke, compression ratio, the number of nozzles, mass flow, and coolant temperature, etc. are determined based on the real experimental data. The main parameters of the modeling are listed in Table 2, which are based on the actual measured values.

The fuel flow is adjusted by the fuel mass injection by the injector in this case the injected diesel to the cylinder is 31.3 mg/cycle and the controlling measures are implemented by regulating the initial gas composition via A/F ratio and the combustion products. The classic species transport is selected for the cycle simulation where the BOOST gas properties tool is used for defining different fuel types properties with different fractions.

The AVL Boost model assembly line of the engine with connected components through pipes is illustrated in Figure 3. The cycle simulation by the software is characterized by the classic species transport method and the spatial discretization of pipes that have an average cell size of 25 mm. This platform supplies an inclusive species transport in full flexibility to deal with the fuel composition and working gas. This is accomplished with an internal solver for chemical reactions. The modeling task is based on the cycle simulation controlled by the classic species transport for the gas exchange and the internal gas properties data file is used therein the enthalpy/entropy values are interpreted by the polynomial coefficients. The cycle type is 4-stroke and the engine runs at 1500 rpm.

In order to guarantee the accuracy of the modeling by software, the heat release rate (HRR), pressure, and temperature of in-cylinder curves are compared in Figure 4. As shown, the validity of the numerical results can be confirmed due to the negligible discrepancy between experimental and numerical values. The highest deviation occurs at 363 CA, which can be attributed to the uncertainty of heat loss and the amount of blow-by from the piston-cylinder configuration.

Upon validation, the tests with different fuels of methane, hythane, and hydrogen blends with diesel are applied in the engine. Then, 10% of water was added to each blended sample to configure their influence on the engine performance. The various blends of fuel composition in the present research together with their specifications are summarized in Table 3. Furthermore, the effects of operational parameters such as engine speed, nozzle diameter, number of nozzle holes, and compression ratio on engine performance and emissions concentration are analyzed.

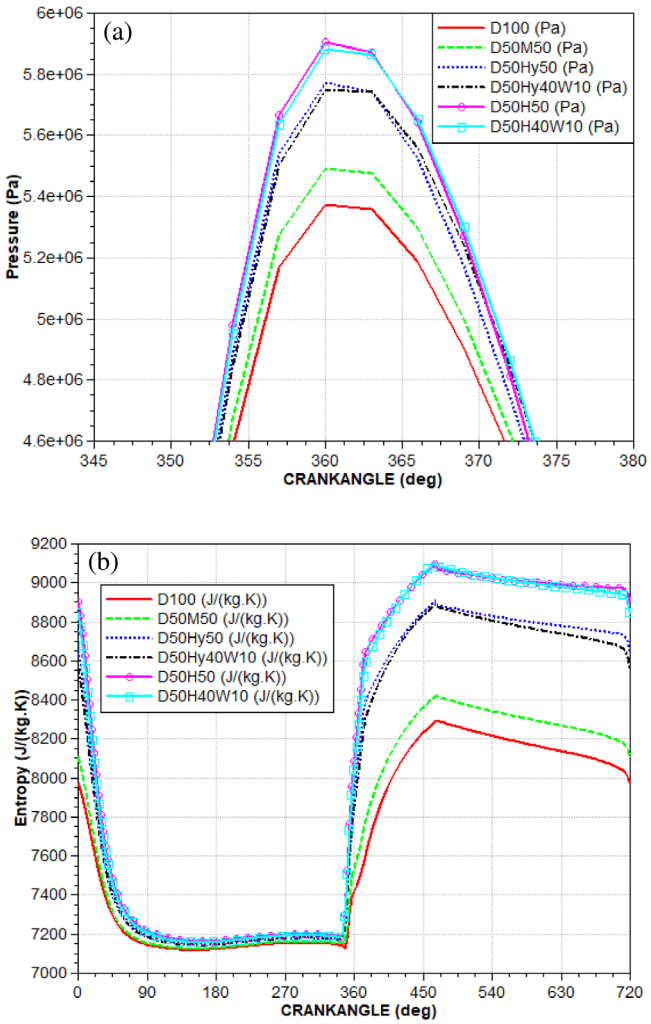

FIGURE 5 (a) Pressure variation and (b) entropy variation with CA for different fuels at the base mode operation

5 | RESULT AND DISCUSSION

The general trend of pressure, entropy, NO_x, and soot emissions with CA are presented in the first section, to provide a clear insight into the effect of fuel composition effect on general engine function. Entropy is a thermodynamic property that plays an important role in the analysis of the system from the second law view and to determine

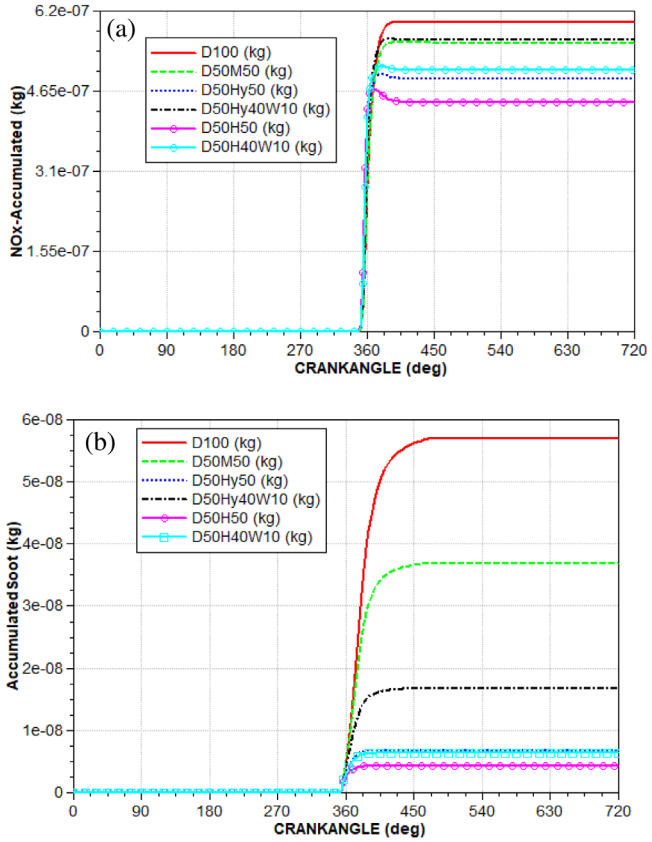

FIGURE 6 (a) Accumulated NO_x and (b) accumulated soot variation with CA for different fuels at the base mode operation

the sources of irreversibilities.[25] The basic values of operational parameters are fixed for the base case, which is CR = 17.5, the number of injector holes = 6, hole diameter = 0.5 mm, and engine speed = 1500 rpm. The variation of the pressure, entropy, NO_x, and soot with crank-angle are demonstrated at the base values. In the next section, the effect of operational parameters on the overall engine performance and emissions are addressed as well to ascertain which fuel is more pragmatic for the particular operational mode.

Figure 5 presents the variation of in-cylinder pressure and entropy with respect to CA for different fuels. In Figure 5a, the pressure at each CA becomes higher in the order of methane, hythane, and hydrogen addition to the base diesel. This can be explained by the thermodynamic properties listed in Table 3, where the A/F ratio and LHV for the compound fuels are increasing in the same order. As the A/F ratio of diesel increases from 15.16 to 24.72 of D50H50 (very lean mixture), it is seen that the peak pressure subsequently increases over 9.89%. The addition of 10% water for hythane and hydrogen blends can slightly reduce the in-cylinder pressure because of the heat absorption of water. According to Figure 5b, the methane, hythane, and hydrogen addition to diesel can gradually increase the entropy generation, since their respective heating value is also increasing. Therefore, when increasing the heating value from 42.8 MJ/kg for diesel to 81.4 MJ/kg for D50H50, the heat loss from the exhaust valve and cylinder wall increases, contributing to entropy increase and irreversibility. Water involvement in the composed fuel leads to both negligible pressure and entropy reduction of as much as 0.4%, which is attributed to steam transferring some of the waste heat. The decrease in peak pressure with 10% water emulsion is in agreement with the results reported in[26] for a biodiesel-diesel-powered CI engine.

Over the emission control strategy, the accumulated NO_x and soot species variations with the fuel blend are exhibited in Figure 6. It is noted that adding methane, hythane and hydrogen fraction to diesel lowers the concentration of NO_x production in the cylinder. Although, the temperature increases with the addition of the gaseous fuel (this can accelerate the forward reaction of the Zeldovich mechanism[27] toward more accumulation of NO_x), the lean mixture formation along with lower oxygen content of hythane and hydrogen justifies the NO_x reduction. The low-level addition of 10% water raises the NO_x amount that is not reported in other scientific reports. A probable cause for this observation is the improvement in spray characteristics with water involvement when there is hydrogen in the fuel blend.

Soot emission is the main challenge for diesel engines that are initiated at rich premixed flames and oxidized at stoichiometric or lean regions. The oxidation rate depends on the OH radicals and high-temperature zones to be oxidized during a long enough residence time.[28] Figure 6b demonstrates a reduction trend of accumulated soot with methane, hythane, and hydrogen addition to diesel. This is mainly due to the formation of a leaner mixture with hydrogen, along with higher temperature and thus oxidation rate that occurs with hydrogen and methane gases introduction. On the other hand, hydrogen and methane have comparatively lower and zero-carbon in their molecular structure, such that the molar mass of diesel ~100 kg/kmol reduces to ~50 kg/kmol for D50H50 (see Table 3).

Figure 7 displays the effect of engine speed on engine performance and exhausted species emissions for different tested fuels. Beginning from Figure 7a, it is evident that engine speed increment leads to an obvious increase in BSFC, while the BMEP tends to a decrease. The pure diesel and diesel–methane samples combustion give the highest fuel consumption rate. As seen, the application of hydrogen and methane (or hythane in the combination form) is effective in lowering the amount of fuel consumption during all engine speed run. The reason is that for sustaining the engine power at a constant level, the hydrogen and methane-involved fuels require lower molar mass to meet the demanded energy (LHV). As a result, an average of 2.1% decrease with methane and a 13.6% decrease of BSFC with hydrogen use occur. Accordingly, the indicated torque and peak burning temperature for different fuels are investigated with respect to the engine speed in Figure 7b. The maximum burning temperature happens at 2500 rpm, while IT reduces steadily with engine speed. The highest value of burning temperature is achieved by D50H50 combustion and the lowest value is attributed to pure diesel (D100). Adding either methane or hydrogen can progressively increase the heating value of the blended fuel, meanwhile, 10% by volume water addition led to ~800 K temperature reduction at 2500 rpm. By increasing the gas (methane/hythane/hydrogen) ratio, the burning rate increases, and thus the mean in-cylinder pressure rise that is conducive to higher torque delivery.

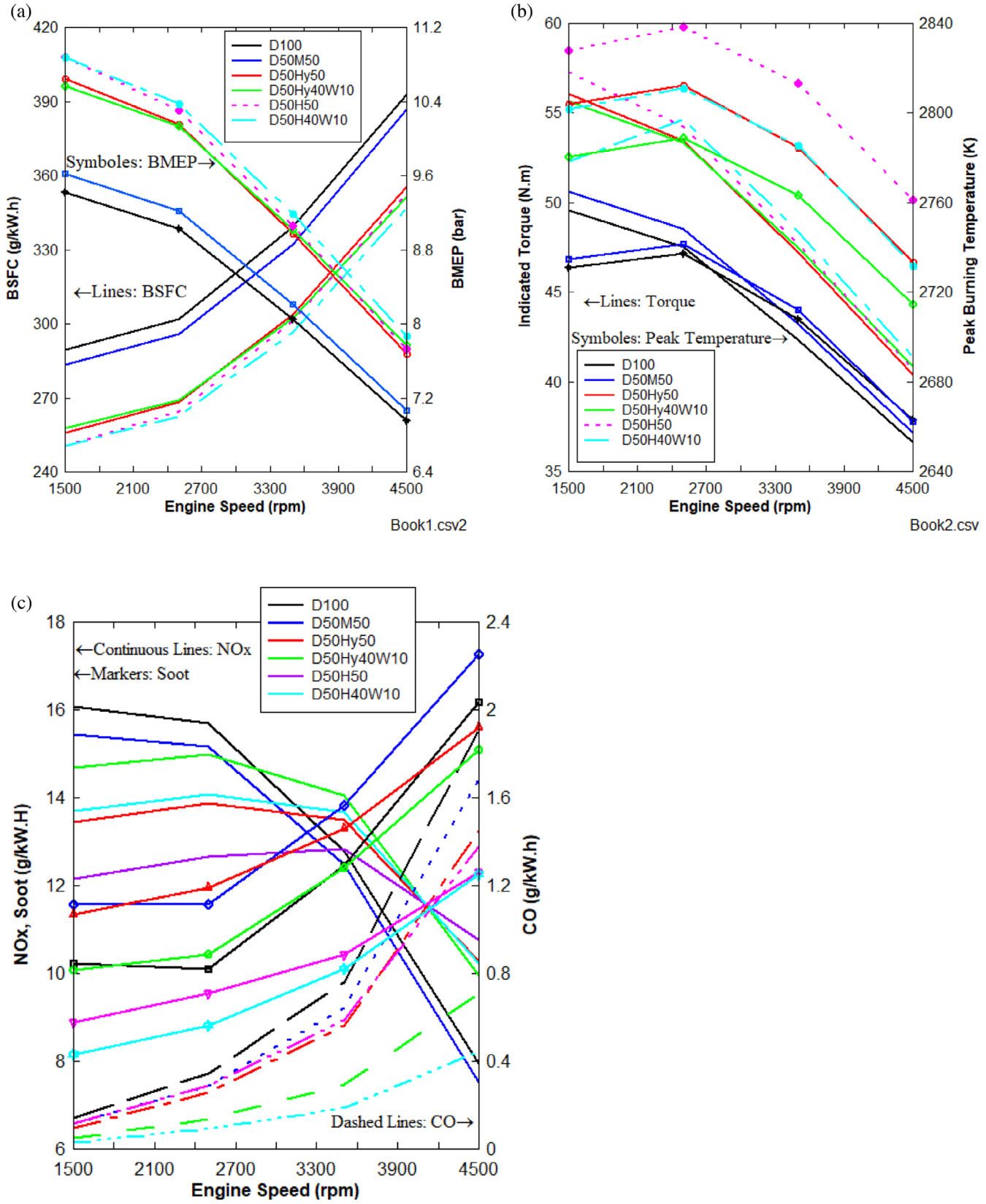

FIGURE 7 The effect of engine speed on (a) BSFC and BMEP, (b) IT and peak burning temperature, and (c) NO_x, CO, and soot for different fuels

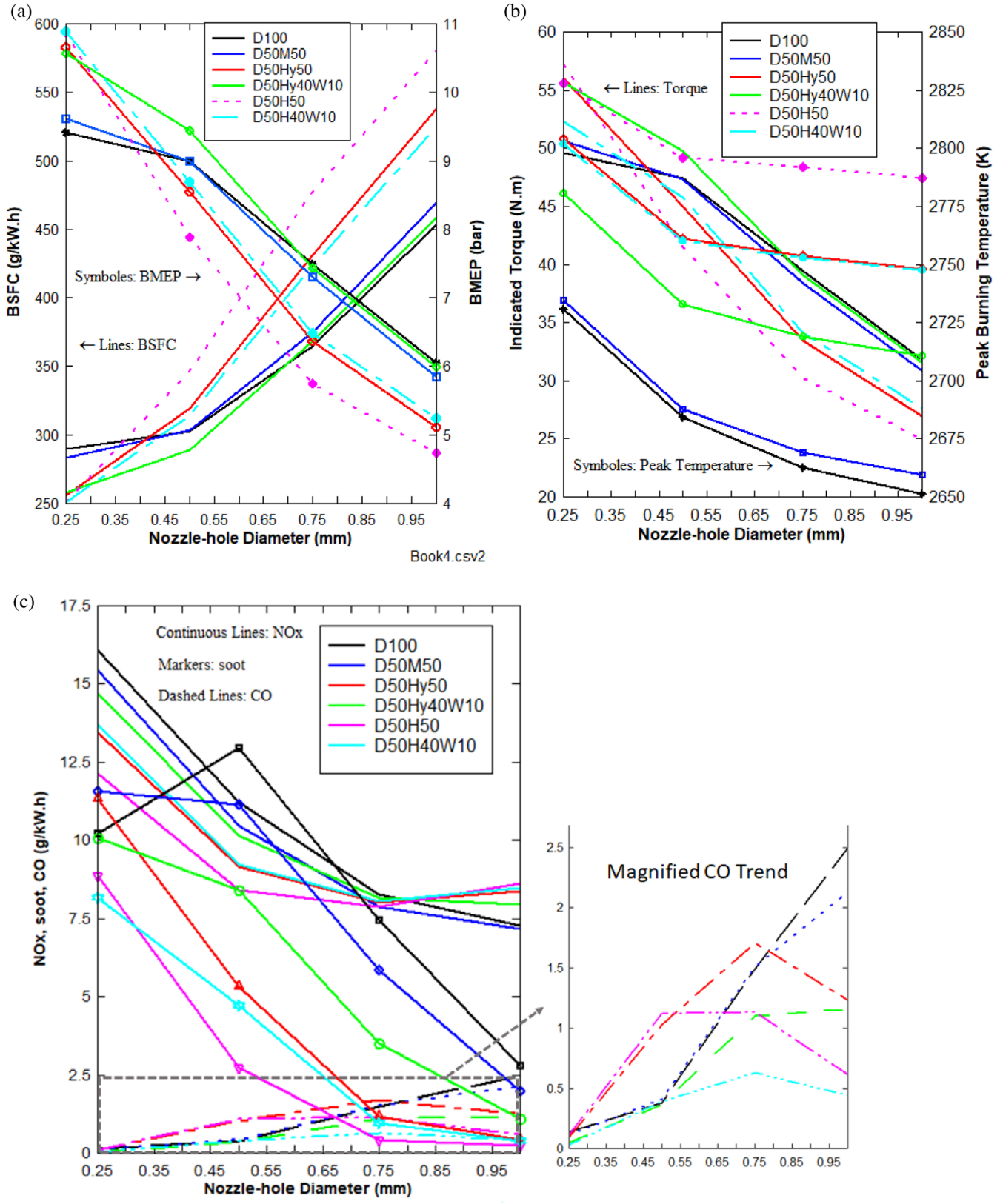

FIGURE 8 The effect of nozzle-hole diameter on (a) BSFC and BMEP, (b) IT and peak burning temperature, and (c) NO_x, CO, soot for different fuels

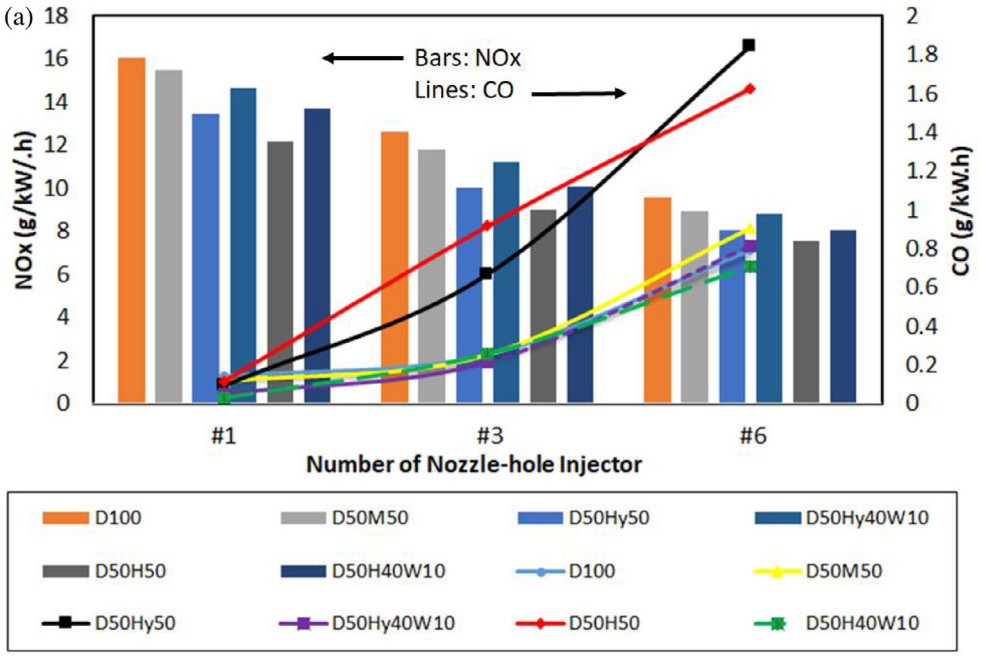

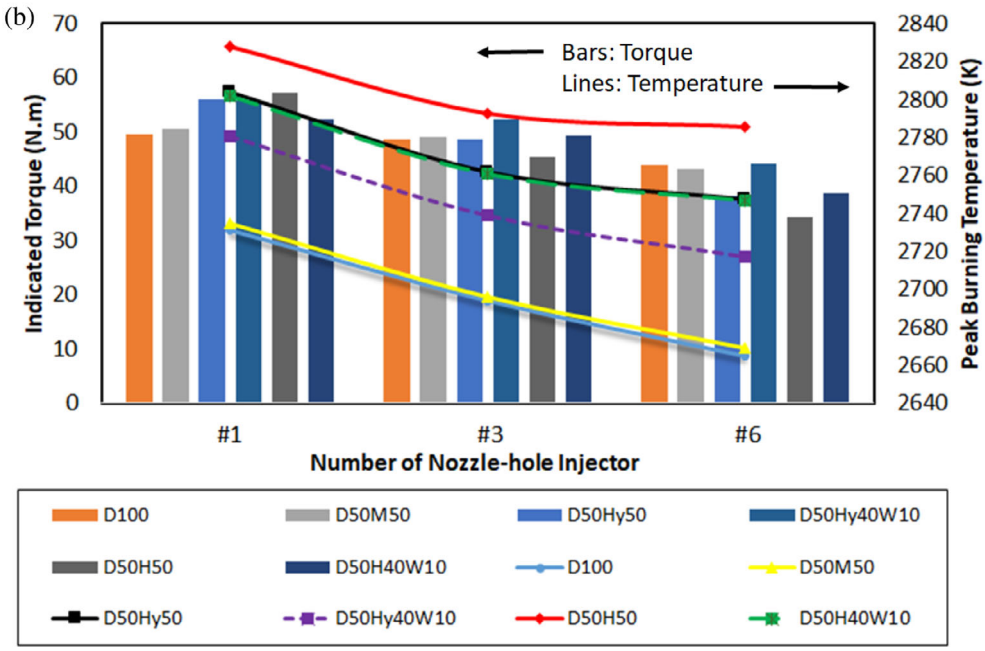

FIGURE 9 (a) NO_x and CO concentration, (b) peak burning temperature and IT variations with number of nozzle hole for different fuels

According to Figure 7c, the average concentrations of NO_x, soot, and CO for different fuel compositions at different engine speeds are recognized. Soot and CO amounts rise with engine speed especially above 2500 rpm, whereas NO_x drops with increasing engine speed. At higher engine speeds, the time for complete combustion shortens, which is the main reason for soot and CO formation. Considering CO and soot, there is a noticeable reduction of these species for D50H40W10 compared to D100 since the carbon-free hydrogen gas is added by 50% with diesel. The NO_x emission shows different behaviors for different fuels at engine speeds lower and higher than 2500 rpm. The NO_x amount falls with the addition of methane, hythane, and hydrogen, however, at higher engine speeds the inverse trend is detected. The decrease of NO_x with H_2 at 1900 rpm and 2500 rpm has been previously reported in Reference 29, where hydrogen+diesel is not increasing the combustion intensity. The addition of H2 to diesel decreases the ignition delay and heat release during the pre-mixed phase, contributing to lower NO_x.[30] The higher NO_x with methane, hythane, and hydrogen application is attributable to more heat generation due to the greater heating value of the gaseous fuels, thereby elevating in-cylinder temperature.

The diameter of the injector determines the cavitation flow regime and the spray breakup and atomization,[31] hence the air–fuel

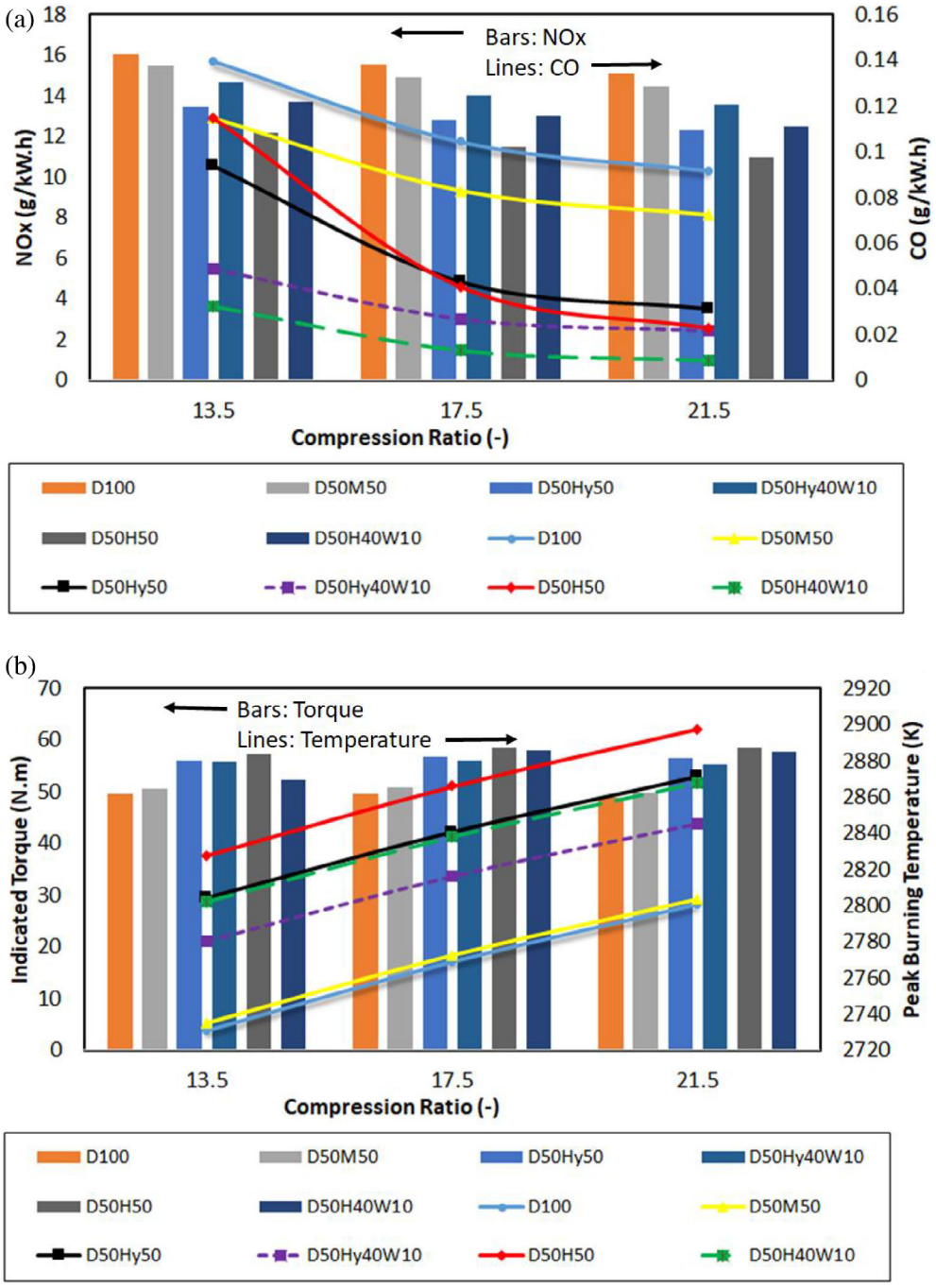

FIGURE 10 (a) NO_x and CO concentration, (b) peak burning temperature and IT variations with compression ratio for different fuels

mixture and subsequent combustion take a drastic effect accordingly. Figure 8a presents the variation of BSFC and BMEP with the nozzle diameter. As the nozzle diameter increases, the fuel consumption increases since more fuel flows through the nozzle. The increase of methane and hydrogen gas share in the diesel contributes to the increase in BSFC since the addition of gaseous fuel portion increases the dual-fuel mass flow rate, while the addition of water, in contrast, reduces the mass flow and hence the BSFC. The fuel consumption for D50H50 is the greatest when the nozzle is large, while for a smaller nozzle, diesel fuel shows more BSFC compared to other fuels. The fuel consumption difference between D50H50 and D100 increases from 14% at a 0.5 mm nozzle hole to 28% at a 1 mm hole diameter due to the increased calorific value of gaseous fuel.[32]

Figure 8b demonstrates that when the nozzle size increases both peak temperature and torque decrease. This is an obvious outcome of deteriorated injection and spray quality at a big nozzle hole disrupting the effective atomization process and making the non-uniform mixture. As a result, fuel evaporation and combustion occur undesirably. Therefore, nozzle diameter increment leads to lower temperature as well as lower engine torque. The maximum peak burning temperature at any hole diameter is associated with D50H50 with 2828 K at 0.25 mm nozzle diameter and base diesel (D100) presents the lowest temperature among the tested blends. Concerning IT, the

D50Hy40W10 is dominant particularly at the lower range of the nozzle hole, while the torque of D50H50 case is noticeably lowest. Further, one can observe that adding water to the compound fuel is contributing toward more engine torque output, although the peak temperature falls with 10% water involvement. The water in the blend absorbs the heat and therefore the combustion temperature is diminished, meanwhile, the generated steam exerts more pressure on the piston and induces a greater torque (~17% increase at 1 mm hole diameter for diesel-hythane case).

Figure 8c shows the emissions concentration for different compound fuels under various nozzle hole diameters. As a general trend, NO_x and soot decrease, while CO increases, with nozzle hole diameter. The addition of gaseous fuels increases CO. The D50H40W10 and D50Hy40W10 cases show the lowest CO content because (1) CH4 and H2 have comparatively lower carbon than diesel in their structures and (2) steam dilution accelerates the third body collision and OH radical formation due to higher pressure, which ultimately decreases the CO content.[33,34] The results indicate that with a small nozzle, NO_x increases with steam dilution. Since the prompt pathway is dominated by a large nozzle, NO_x decreases with water due to the thermal NO_x effect. The increase of gaseous fuel portion in diesel brings about a significant reduction of soot since the hydrogen and methane burn without smoke and the temperature increase would oxidize the soot, thus soot amount further decreases with methane, hythane, and hydrogen successively. On the other hand, 10% water in the blend is seen to decrease the soot loading at 0.25 mm nozzle diameter where the spray structure has better quality and jet disintegration is implemented efficiently. At larger hole diameters, the reverse trend can be discerned when water is involved, affecting the soot content adversely since water promotes soot surface growth and the extent of carbonization, reduces slightly the soot oxidation.[35] It is believed that when using a small nozzle, the tiny droplets of water are evaporated easily and the steam controls the soot formation via dilution and chemistry (mostly through the backward $OH + H2 \leftrightarrow H + H_2O$ pathway[36]).

The number of nozzle holes in the injector with a fixed injection rate and mass flow is investigated on the engine performance and main pollutant emissions. Figure 9a shows NO_x and CO emissions concentration for different analyzed fuels as a function of the number of holes. Overall, increasing the number of holes from 1 to 6 yields an average 40% drop in NO_x, which comes from lower injection pressure and velocity, poor mixture formation, deficient combustion, and lower temperature; consequently, NO_x decreases (the results are in agreement with results of[37]). Next, CO increases considerably with the number of nozzle holes due to the incomplete combustion mentioned above. The practical role of gaseous fuels (hydrogen, hythane, and methane) on NO_x and CO engine-out content can be appreciated again.

As seen from Figure 9b, increasing the number of nozzle holes brings about both peak temperature and indicated torque reduction; for example, the D50H50 peak temperature is decreased from 2828 K to 2792 K to 2785 for 1, 3, and 6 holes, respectively. Similarly, IT values are decreasing with increasing hole number since for a fixed hole area, fuel is injected with lower velocity, and uniform air–fuel formation deteriorates, worsening engine performance, especially for D50H50 (~40% reduction). It is noteworthy that IT reduction with nozzle hole number affects D50H50, while its impact on D100 is insignificant.

Figure 10a shows that NO_x is gradually decreasing with increasing compression ratio, and water involvement caused NO_x to increase. The amount of CO is also continuously decreasing with compression ratio as a higher compression ratio is attributable to more complete combustion and more CO to CO_2 oxidation rate. The addition of methane, hythane, and hydrogen further reduced CO, while water involvement intensifies the CO emission reduction.

The engine performance and combustion parameters of IT and peak temperature are graphed for different fuels under different compression ratio levels in Figure 10b. The maximum temperature and torque are associated with D50H50. In addition, water emulsion contributed to a slight torque reduction and marked peak temperature decrease in all studied compression ratios.

6 | CONCLUSION

A numerical investigation is carried out to analyze the powertrain performance and the following points are summarized:

- The peak pressure increases when blending methane, hythane, and hydrogen with diesel accordingly. This is due to higher flame speed and better mixture uniformity of hydrogen and methane. Injecting water slightly reduces the peak pressure.
- Hydrogen and methane can reduce the soot emission due to no/fewer carbon compared to diesel (5 times lower soot emission by D50H50). However, the injected water gives heightened soot since the oxidation rate is reduced.
- The combustion temperature for all fuel compositions peaks at 2500 rpm and the highest temperature of 2840 K is associated with D50H50. Increasing the nozzle hole diameter results in the indicated torque drop of up to 50% for D50H50.
- For a fixed nozzle opening area, increasing the number of the hole is not recommended. The highest IT with one nozzle hole is for D50H50 (57.25 N m), with 6 nozzle holes, and the lowest torque occurs with D50H50 (34.13 N m).
- The amount of entropy significantly increased for D50H50 and D50Hy50 compared to D100 since methane and hydrogen both produce a high rate of thermal energy that dissipates through chamber walls into the environment.

AUTHOR CONTRIBUTIONS

Hadi Taghavifar: Conceptualization (lead); data curation (lead); formal analysis (lead); investigation (lead); methodology (lead); project administration (lead); resources (lead); software (lead); supervision (lead); validation (lead); visualization (lead); writing—original draft (lead); writing—review and editing (lead).

DATA AVAILABILITY STATEMENT

Author elects to not share data.

ORCID

Hadi Taghavifar https://orcid.org/0000-0002-8793-7140

REFERENCES

1. IEA. *CO_2 Emissions from Fuel Combustion 2016*. IEA; 2016. doi:10.1787/co2_fuel-2016-en
2. Bao LZ, Sun BG, Luo QH, Wang X, Niu QY. Experimental study of the polytropic index of the compression stroke for a direct injection hydrogen engine. *Int J Hydrogen Energy*. 2020;45:28196-28203.
3. Amirante R, Cassone E, Distaso E, Tamburrano P. Overview on recent developments in energy storage: mechanical, electrochemical and hydrogen technologies. *Energ Conver Manage*. 2017;132:372-387.
4. Taghavifar H, Anvari S, Parvishi A. Benchmarking of water injection in a hydrogen-fueled diesel engine to reduce emissions. *Int J Hydrogen Energy*. 2017;42(16):11962-11975.
5. Changizian S, Ahmadi P, Raeesi M, Javani N. Performance optimization of hybrid hydrogen fuel cell-electric vehicles in real driving cycles. *Int J Hydrogen Energy*. 2020;45:35180-35197.
6. Sandalcı T, Işın Ö, Galata S, Karagöz Y, Güler İ. Effect of hythane enrichment on performance, emission and combustion characteristics of an ci engine. *Int J Hydrogen Energy*. 2019;44(5):3208-3220.
7. European Environment Agency. 2016. EMEP/EEA Air Pollutant Emission Inventory Guidebook 2016: technical guidance to prepare national emission inventories. *EEA-Report*, p. 21.
8. Hydrogen Fuel Cell Vehicles. https://www.epa.gov/greenvehicles/hydrogen-fuel-cell-vehicles
9. Karim GA. Hydrogen as a spark ignition engine fuel. *Int J Hydrogen Energy*. 2003;28(5):569-577.
10. Yan F, Xu L, Wang Y. Application of hydrogen enriched natural gas in spark ignition IC engines: from fundamental fuel properties to engine performances and emissions. *Renew Sustain Energy Rev*. 2018;82:1457-1488.
11. Gong C, Li Z, Chen Y, Liu J, Liu F, Han Y. Influence of ignition timing on combustion and emissions of a spark-ignition methanol engine with added hydrogen under lean-burn conditions. *Fuel*. 2019;235:227-238.
12. Yip HL, Srna A, Yuen ACY, et al. A review of hydrogen direct injection for internal combustion engines: towards carbon-free combustion. *Appl Sci*. 2019;9(22):4842.
13. Taghavifar H, Mazari F. 1D diesel engine cycle modeling integrated with MOPSO optimization for improved NO_x control and pressure boost. *Energy*. 2022;247:123517.
14. Taghavifar H, Nemati A, Salvador FJ, De la Morena J. 1D energy, exergy, and performance assessment of turbocharged diesel/hydrogen RCCI engine at different levels of diesel, hydrogen, compressor pressure ratio, and combustion duration. *Int J Hydrogen Energy*. 2021;46(42):22180-22194.
15. Subramanian B, Lakshmaiya N, Ramasamy D, Devarajan Y. Detailed analysis on engine operating in dual fuel mode with different energy fractions of sustainable HHO gas. *Environ Prog Sustain Energy*. 2022;e13850. doi:10.1002/ep.13850
16. Karagöz Y, Balcı Ö, Köten H. Investigation of hydrogen usage on combustion characteristics and emissions of a spark ignition engine. *Int J Hydrogen Energy*. 2019;44(27):14243-14256.
17. Ayad SM, Belchior CR, da Silva GL, Lucena RS, Carreira ES, de Miranda PE. Analysis of performance parameters of an ethanol fueled spark ignition engine operating with hydrogen enrichment. *Int J Hydrogen Energy*. 2020;45(8):5588-5606.
18. Niculae AL, Miron L, Chiriac R. On the possibility to simulate the operation of a SI engine using alternative gaseous fuels. *Energy Rep*. 2020;6:167-176.
19. Xu P, Ji C, Wang S, et al. Effects of direct water injection on engine performance in engine fueled with hydrogen at varied excess air ratios and spark timing. *Fuel*. 2020;269:117209.
20. Saraee HS, Jafarmadar S, Sayadi M, Parikhani A, Kheyrollahi J, Pourvosoughi N. Green fuel production from Pistacia Khinjuk and its engine test analysis as a promising alternative. *J Clean Prod*. 2017;156:106-113.
21. Boost A. Theory manual (AVL boost v.2018.1), AVL list Gmbh, Graz-Austria, 2018.
22. Woschni G. Einfluß von Rußablagerungen auf den Wärmeübergang zwischen Arbeitsgas und Wand im Dieselmotor. *Proceedings to Der Arbeitsprozeß des Verbrennungsmotors*; 1991.
23. Chmela FG, Orthaber GC. Rate of heat release prediction for direct injection diesel engines based on purely mixing controlled combustion. *SAE Trans*. 1999;152-160.
24. Chmela F, Orthaber G, Schuster W. Die Vorausberechnung des Brennverlaufs von Dieselmotoren mit direkter Einspritzung auf der Basis des Einspritzverlaufs. *MTZ-Motortechnische Z*. 1998;59(7–8):484-492.
25. Moran MJ, Shapiro HN, Boettner DD, Bailey MB. *Fundamentals of Engineering Thermodynamics*. John Wiley & Sons; 2010.
26. Maawa WN, Mamat R, Najafi G, De Goey LPH. Performance, combustion, and emission characteristics of a CI engine fueled with emulsified diesel-biodiesel blends at different water contents. *Fuel*. 2020;267:117265.
27. Zeldovich YA, Frank-Kamenetskii D, Sadovnikov P. *Oxidation of Nitrogen in Combustion*. Publishing House of the Acad of Sciences of USSR; 1947.
28. McAllister S, Chen JY, Fernandez-Pello AC. *Fundamentals of Combustion Processes*. Vol 302. Springer; 2011.
29. Juknelevičius R, Rimkus A, Pukalskas S, Matijošius J. Research of performance and emission indicators of the compression-ignition engine powered by hydrogen-diesel mixtures. *Int J Hydrogen Energy*. 2019;44(20):10129-10138.
30. Lee T, Park J, Kwon S, Lee J, Kim J. Variability in operation-based NO_x emission factors with different test routes, and its effects on the real-driving emissions of light diesel vehicles. *Sci Total Environ*. 2013;461:377-385.
31. Taghavifar H, Anvari S, Mousavi SH. Assessment of varying primary/secondary breakup mechanism of diesel spray on performance characteristics of HSDI engine. *Fuel*. 2020;262:116622.
32. Karagöz Y. Analysis of the impact of gasoline, biogas and biogas+hydrogen fuels on emissions and vehicle performance in the WLTC and NEDC. *Int J Hydrogen Energy*. 2019;44(59):31621-31632.
33. Kobayashi H, Yata S, Ichikawa Y, Ogami Y. Dilution effects of superheated water vapor on turbulent premixed flames at high pressure and high temperature. *Proc Combust Inst*. 2009;32(2):2607-2614.
34. Göke S, Schimek S, Terhaar S, et al. Influence of pressure and steam dilution on NO_x and CO emissions in a premixed natural gas flame. *J Eng Gas Turb Power*. 2014;136(9):V01AT04A056.
35. Ying Y, Liu D. Effects of water addition on soot properties in ethylene inverse diffusion flames. *Fuel*. 2019;247:187-197.
36. Liu F, Consalvi JL, Fuentes A. Effects of water vapor addition to the air stream on soot formation and flame properties in a laminar coflow ethylene/air diffusion flame. *Combust Flame*. 2014;161(7):1724-1734.
37. Kim, BS, Yoon, WH, Ryu, SH and Ha, JS. 2005. Effect of the injector nozzle hole diameter and number on the spray characteristics and the combustion performance in medium-speed diesel marine engines (No. 2005-01-3853). SAE Technical Paper.

How to cite this article: Taghavifar H. Experimental and numerical engine cycle setup for a dual fuel hydrogen, methane, and hythane with diesel to assess the effect of water injection and nozzle geometry. *Environ Prog Sustainable Energy*. 2022;e13936. doi:10.1002/ep.13936